Mechanisms of spatiotemporal selectivity in cortical area MT

Ambarish S. Pawar,[1,*] Sergei Gepshtein,[1] Sergey Savel'ev,[2] Thomas D. Albright [1]

[1] Systems Neurobiology Laboratories, The Salk Institute for Biological Studies, La Jolla, CA 92037, USA
[2] Department of Physics, Loughborough University, Loughborough LE11 3TU, United Kingdom

* Corresponding author: *ambarish@salk.edu*

Summary

Cortical sensory neurons are characterized by selectivity to stimulation. This selectivity was originally viewed as a part of the fundamental "receptive field" characteristic of neurons. This view was later challenged by evidence that receptive fields are modulated by stimuli outside of the classical receptive field. Here we show that even this modified view of selectivity needs revision. We measured spatial frequency selectivity of neurons in cortical area MT of alert monkeys and found that their selectivity strongly depends on luminance contrast, shifting to higher spatial frequencies as contrast increases. The changes of preferred spatial frequency are large at low temporal frequency and they decrease monotonically as temporal frequency increases. That is, even interactions among basic stimulus dimensions of luminance contrast, spatial frequency and temporal frequency strongly influence neuronal selectivity. This dynamic nature of neuronal selectivity is inconsistent with the notion of stimulus preference as a stable characteristic of cortical neurons. [150 of 150 allowed]

Introduction

One of the most important questions in neuroscience today concerns the mechanisms by which sensory systems manifest selectivity for specific attributes of the sensory stimulus. This question has been addressed most extensively for the visual modality and has been posed in many different forms: What accounts, for example, for the limited range of visual sensitivities to luminance and chrominance, or to the spatial and temporal properties of an image, or to the types of faces we can best discriminate? The question of selectivity also concerns the core concept of the neuronal *receptive field*, used to describe what sensory properties neurons prefer, how and why they develop such preferences, and how neurons contribute to perceptual experience.

The classical conception of the visual receptive field is a characteristic of the neuron defined in terms of stimuli that elicit the neuron's response, including the spatial region of stimulation and other stimulus dimensions, such as orientation, spatiotemporal frequency, and

direction of movement. A neuron's sensitivity to each dimension is quantified by a "tuning function" that describes the range of parameters that activate the neuron.

The classical conception was revised when neuronal responses were found to depend on properties of stimuli falling outside of the classical receptive field (CRF) (Bishop et al., 1973; Allman et al. 1985; Tanaka et al., 1986). Effects induced by stimuli in the larger "non-classical" receptive field (nCRF) enable neurons to interpret and organize image features by taking into account the larger spatial context in which they appear (e.g., Das & Gilbert, 1999; Albright and Stoner, 2002; Li et al., 2006). In this revised view, neuronal responses to stimuli within the CRF are believed to depend on feedforward connections (Hubel & Wiesel, 1962; Mountcastle, 1957; Barlow, 1972; DeValois et al., 1982; Movshon et al., 1978), whereas stimuli outside of the CRF are thought to play a modulatory role, by means of lateral and feedback connections.

Rapidly growing evidence makes it clear, however, that effects of contextual interactions on neuronal selectivity are even more pervasive than suggested by the early studies of nCRF. For example, tuning to stimuli presented within CRF was found to depend on the stimulus "context" construed broadly: not only as a larger spatial surround of CRF, but as a nonlinear interaction of stimulus dimensions. Indeed, even effects of stimuli presented entirely within the CRF are often "inseparable" (e.g., Fleet et al., 1985; Dong, 2001, Albright & Stoner, 2002; Huang et al. 2007; Priebe et al., 2006; Albright, 2012, 2015) in that the neural response cannot be predicted in terms of linear combination of the effects of these dimensions measured in isolation. In particular, the tuning of cortical neurons to motion direction and spatial frequency of the stimulus was shown to depend on the stimulus luminance contrast in cortical area V1 in the monkey (Albrecht 1995; Sceniek et al., 2002; Priebe et al., 2006), in the cat (Holub & Morton-Gibson, 1981), and in the ferret (Rubin et al., 2015). Similar results were found in area MT of alert monkey, where the tuning to direction of motion and motion speed also depended on contrast (Pack et al., 2005). Here we seek to shed more light on the nature of circuit interactions that shape cortical selectivity. We investigate tuning of individual cortical cells to several stimulus dimensions, with a focus on how tuning depends upon interactions between these dimensions.

We studied the tuning of single neurons in the middle temporal (MT) cortical area of awake macaque monkey. Area MT plays a fundamental role in spatiotemporal vision and motion perception, and MT neurons have been shown to be susceptible to contextual modulations (Allman et al., 1985; Priebe et al., 2006; Stoner & Albright, 1992; Duncan et al., 2000; Huang et al., 2007; Schlack & Albright, 2007). We measured the tuning of single cortical cells to SF of drifting luminance gratings, in which we varied spatial frequency, temporal frequency, and luminance contrast. We found that SF tuning of cortical neurons changes as a function of both

contrast and temporal frequency. The observed changes in tuning to SF were significantly larger than those observed in previous studies of area V1 (Sceniak et al., 2002 in old world monkeys; Rubin et al., 2015 in the ferret) in anesthetized animals. Such changes in selectivity of MT neurons are evidence of nonlinear interactions between three basic stimulus dimensions: luminance contrast, spatial frequency and temporal frequency. This dynamic nature of neuronal selectivity is inconsistent with the notion of stimulus preference as a stable characteristic of cortical neurons.

RESULTS

Changes in spatial frequency tuning of MT neurons across contrasts

To understand how neuronal tuning changes across contrasts, we derived neuronal response surfaces for individual neurons. A response surface is the firing rate of a neuron plotted as a function of two stimulus parameters, here spatial frequency (SF) and luminance contrast. Such response surfaces serve as useful summaries of neuronal selectivity. One such surface for an MT neuron is shown at left in Figure 1A. The firing rate of this neuron is plotted as a function of five values of SF measured at seven stimulus contrasts.

A vertical slice of the response surface, parallel to the axes of firing rate and SF, is a *spatial response function*. One such function is shown at right in Figure 1A. This function describes how the firing rate of the neuron varies across SF at a single stimulus contrast (here 17.1%). Such response functions are commonly used to capture suprathreshold behavior of cortical neurons (e.g., Movshon et al., 1978; Priebe et al., 2003; Sceniak et al., 2002; Krekelberg et al., 2006).

Each neuron can be characterized by multiple spatial response functions at different stimulus contrasts, as shown in Figure 1B-D for three different neurons. In each panel, the upper edge of the shaded region represents the threshold firing rate defined as one standard deviation above the resting firing rate. The three neurons manifest three qualitatively distinct types of behavior observed in our data. For the neuron in Figure 1B, the SF of maximal response (henceforth “peak response”) shifted strongly to higher SF with increasing contrast, such that the peak response at 100% contrast (1 c/deg) is ~8 times that of the 7% contrast (0.12 c/deg). For another neuron, in Figure 1C, the peak responses did not change with contrast. And for the neuron in Figure 1D, peak responses shifted with contrast toward lower spatial frequencies. Collectively, these data demonstrate that SF tuning characteristics of MT neurons vary as a function of stimulus contrast; peak responses shift to high spatial frequencies (Figure 1B), do not change (Figure 1C), or shift to low spatial frequencies (Figure 1D).

We studied how peak responses changed with contrast across the population of all recorded neurons: 74 neurons in Monkey 1 and 65 neurons from Monkey 2. For the entire population of recorded neurons, responses were measured at six spatial and eight temporal frequencies (TF). Figure 2 is a plot of stimulus sampling for every measured spatiotemporal frequency in both monkeys. Circle sizes represent the number of measurements performed at each spatiotemporal frequency. The marginal distributions of sampling stimulus frequencies are also shown. Overall, we sampled a large portion of the visible spatiotemporal stimulus space in both monkeys (Pawar A.S., Laddis P., Gepshtein S., Albright T.D. Rapid measurement of spatiotemporal contrast sensitivity in behaving macaque monkeys. Program No. 458.16. *2013* Neuroscience Meeting Planner. San Diego, CA. Society for Neuroscience, 2013, online).

To understand how peak responses changed with contrast across the entire population of measured neurons, we normalized stimulus SF by setting the peak response at 100% contrast to unity for all neurons and then traced peak SFs across contrast (Figure 3). To help intuition, in Figure 3A we have plotted five response functions from one recorded neuron, in which the peak response shifted to high SFs. The three numbered disks represent peak responses at the three highest contrasts tested. At the two highest contrasts (100% and 30%) the peak responses marked by disks 1 and 2 are for SFs of 1 and 0.25 c/deg respectively. Disk 3 marks the peak response at the contrast for which firing rate just exceeds threshold, which for this neuron was 7%. Here, the peak SF is 0.12 c/deg. The magnitude of SF shift was quantified by normalizing to peak response at the highest contrast (as explained above) and then computing the log ratio of peak responses.

In Figure 3B, results of this analysis are shown for four representative neurons in Monkey 1 (top row) and Monkey 2 (bottom row). The lines in each panel connect values of normalized peak SFs across contrasts; the three lines correspond to three TFs measured for each neuron. The shaded bands for each line represent 95% confidence intervals of peak responses estimated using the resampling procedure described in section *Quantification and statistical analysis of* Methods. The numbered disks in the bottom left panel in Figure 3B correspond to the disks shown in Figure 3A. For the conditions marked by disks 2 and 1 in Figure 3A, the log ratio of peak responses is -0.6, and for the conditions 3 and 1, the log ratio of peak responses is -0.92. In other words, in this neuron peak responses changed with contrast to higher SF. Such drifts of neuronal preference toward higher or lower spatial frequencies are represented respectively as leftward or rightwards trajectories across contrast emanating from a single point on the dimension of normalized SF. Overall, Figure 3B illustrates a range of neuronal behavior: drift of preference to high SF (left panels), low SF or no change (right panels).

The drift of preference for all recorded MT neurons (N=139) in two monkeys are plotted in Figure 3C. Each ascending line represents the trace of peak responses across contrasts for one neuron recorded at a single TF. To recall, peak responses were measured at one to three TFs in each neuron yielding 180 peak responses from 74 neurons in Monkey 1 and 198 peak responses from 65 neurons in Monkey 2. The plots reveal the range of neuronal behaviors we have seen already in Figure 3B; peak responses change with contrast: to lower SF (yielding negative slopes), to higher SF (positive slopes), and in some cases in both directions (positive and negative slopes). The thick black lines represent the geometric mean of all the traces, indicating that the tuning of a large majority of neurons shifted to higher spatial frequencies in both monkeys. (Supplementary Figure S3 illustrates response drifts along with 95% confidence intervals for the entire population of measured neurons.)

Statistical analysis of tuning dynamics

Figure 4 is a summary of peak response variation for three pairs of tested stimulus contrasts, for all neurons and spatiotemporal stimulus conditions, separately for Monkey 1 (A-C) and Monkey 2 (D-F). The “high,” “medium,” and “low” stimulus contrasts used in Figure 4 were 100%, 30% and 7%, respectively. Threshold contrasts were different for different neurons, depending on threshold firing rate, as defined in section *Changes in spatial frequency tuning of MT neurons across contrasts*, represented in Figure 1B-D by the upper edge of the shaded region. Every panel in this figure is a scatter plot of peak responses for two contrasts: high vs. medium, high vs. low and high vs. threshold. Each data point in the scatter plot represents an estimate of peak response within a particular temporal frequency. Henceforth, “case” refers to a single temporal frequency. (In some cases, we were not able to capture the peak of the SF tuning function because the peak was likely to occur at an SF outside the range of SF used to measure response functions. Overall, 56 such cases in Monkey 1 and 98 cases in Monkey 2 were not included in Figure 4 and the statistical analysis described below.) The numbers and percentages of data points on either side of the diagonal, where the compared quantities are identical, are displayed in the top left and bottom right corners of each panel. For both monkeys, only those cases are represented in which peak responses were greater than threshold firing rate. (The number of cases is larger than the number of neurons recorded because, as mentioned, we measured peak responses at one to three TFs from each neuron.)

These plots reveal general trends in the population data. For example, in Figure 4A, the number of points that lie below the diagonal is 27 percentage points greater than the number of

points above the diagonal (60% vs. 33%). This indicates that as contrast increases from medium to high, the number of cases where the peak responses shifts towards higher or lower SF is biased towards shifts to higher SF. This bias grows stronger when we compare shift of peak responses at high vs. low contrasts (73% vs. 27%, Figure 4B) and more so when we compare high vs. threshold contrast (79% vs. 22%, Figure 4C). The results of Figure 4C, where the number of points below the diagonal is more than three times the number of points above, reveal that in a majority of the population, peak SF shifts towards higher rather than lower SF. A similar pattern holds for Monkey 2, where in a majority of the neuronal population, peak responses shift more towards higher than lower SFs at all pairs of contrasts. Here, the number of points below the diagonal is more than twice those above even at high vs. medium contrasts (66% vs. 27%, Figure 4D). This asymmetry becomes even stronger in the comparison of high vs. low contrasts (80% vs. 17%, Figure 4E) and high vs. threshold contrast (85% vs. 16%, Figure 4C). Overall, the peak of SF tuning shifts strongly to higher rather than lower SFs in both monkeys, especially when we compare high and threshold contrasts.

To determine if the changes of tuning were significantly different across contrasts, we performed the Wilcoxon rank-sum test on the resampled data. Results of this analysis are indicated by n^* on the top of all the panels in Figure 4. For Monkey 1, we found a significant difference ($p<0.01$) between peak responses in 81% of cases at high vs. medium contrasts, in 90% of cases at high vs. low contrasts and in 91% of cases at high vs. threshold contrasts. For Monkey 2, we found a significant difference ($p<0.01$) between peak responses in 78% of cases at high vs. medium contrasts, in 85% of cases at high vs. low contrasts and in 88% of the cases at high vs. threshold contrasts. In summary, changes of neuronal preference were highly significant in a majority of cases in both monkeys.

So far, in exploring changes of SF tuning across multiple contrasts, we have ignored the dimension of TF. In the data displayed in Figures 3-4, we made no distinction between the data collected at different TFs. In the next section, we consider how TF affected the relationship between neuronal SF preference and stimulus contrast.

Tuning dynamics and stimulus temporal frequency

In Figure 5, we divided data from one of the contrast comparisons illustrated in Figure 4 (panels C and F) into three frequency bands: high TF (16 and 32 Hz), medium TF (4 and 8 Hz) and low TF (0.25 to 2 Hz). Similar to Figure 4, each data point in the scatter plots represents a pair of estimates of peak SF responses at two contrasts. Data for different monkeys are shown in

different columns. This figure reveals that the main effect reported in the previous section, the change of peak SF with stimulus contrast, is most prominent at low TF. This effect of contrast diminishes as TF increases. That is, the number of data points falling above and below the diagonal is uneven at low TF (Figures 4E and 5F). As TF increases, the numbers of points above and below the diagonal become balanced in both monkeys. In Monkey 1, the fraction of points below the diagonal decreases from 77% at low TF to 57% at medium TF, and then to 50% at high TF. And in Monkey 2, the fraction of points falling below the diagonal decreases from 83% at low TF to 73% at medium TF, and then to 65% at high TF. In summary, TF strongly modulates the influence of contrast on spatial frequency tuning of MT neurons.

The influence of TF on the change of peak SF is summarized for the entire population of neurons in Figure 6. Geometric means of peak SF are plotted for different values of TF for two contrast pairs: 7% vs. 100% in Figure 6A and threshold vs. 100% in Figure 6B. Because a small number of samples were obtained at TF of 0.25 Hz (see Figure S1) for both monkeys, we combined data at TF of 0.25 and 0.5 Hz. The combined data is shown in Figure 6 as a TF of 0.38 Hz. The means of peak SF for all measured neurons for the two monkeys appear in separate rows of plots, revealing two trends that are similar in both monkeys. First, peak SF *increases* with TF at low contrast, represented by open black symbols in Figure 6A and filled black symbols in Figure 6B. Second, peak SF *decreases* with TF at high contrasts, represented by red symbols in Figure 6A-B. Another way to interpret these results is in terms of the magnitude of change in peak SF for different values of TF. The largest SF change is found at low TF. As TF increases, the difference between peak SF at low and high contrasts becomes progressively smaller. The difference is significant at low TF and is not significant at high and medium TF ($p<0.05$, asterisks).

Further statistical details of these analyses are summarized in Figure 7. Similar to Figure 3B, response drifts were calculated as the decimal log ratio of peak responses at two pairs of contrasts: 7% and 100% in Figure 7A, and threshold and 100% in Figure 7B. In both monkeys and both contrast pairs, response drifts are large at low TFs and they monotonically approach zero as TF increases. The histograms at right of each panel represent the number of cases sampled from each TF. Even though *median* response drifts are close to zero at medium and high TFs, *individual* response drifts for many TFs (individual cases) at medium and high TFs can be significantly different form one another, as we have seen in Figure 4. The numbers of such significant individual cases are reported in Figure 7 using the white bars inscribed in the colored histograms. In summary, the results reported in Figure 6-6 demonstrate that stimulus TF strongly modulates the influence of luminance contrast on preferred SF of MT neurons.

DISCUSSION

We investigated cortical mechanisms of sensory selectivity for the stimulus dimensions of spatial and temporal frequency (SF and TF), and how this selectivity depends on stimulus luminance contrast. We studied how SF tuning of cortical neurons depends on stimulus luminance contrast and TF in area MT of two alert macaque monkeys. We found that neurons changed their SF tuning with contrast and that the amount of change depended on stimulus TF. As contrast increased, the preferred SF of neurons shifted, most commonly toward higher than lower SF. The shift size was largest at low TF, and it decreased monotonically as TF increased. In the following, we review our results in the context of previous studies of cortical tuning and consider the role of circuit interactions in shaping cortical tuning.

Role of inhibition in cortical tuning

Previous studies of neuronal SF selectivity in other cortical areas found only small changes of tuning with contrast. Sceniak et al. (2002) measured tuning of neurons across two contrasts levels in cortical area V1 of macaque monkeys. The bandwidth, but not the peak, of SF tuning was found to change. More recently, Rubin et al. (2015) studied SF tuning of neurons in area V1 of ferrets and found small (less than twofold) but significant changes in peak SF across luminance contrasts. Both studies were performed in anesthetized animals. In the present study, we found in alert animals that peak SF of neurons changed as much as tenfold (Figure 6B).

Anesthesia could be one reason for the differences in flexibility of tuning reported here and in previous studies. Anesthesia is known to suppress feedback to V1 from MT and other higher cortical areas (Alkire et al., 2009; Hudetz 2008; Super et al., 2001). Top-down feedback connections are known to be both excitatory and inhibitory, although descending inhibition greatly exceeds descending excitation (e.g., Hupe et al., 1998; Bullier et al., 1996). Overall, cortical inhibition plays an important role in shaping evoked and spontaneous cortical activity (Buzsaki, 2006; Isaacson & Scanziani, 2011). Studies in rodents reveal that anesthesia affects the balance of excitation and inhibition in the cortex, shifting the balance toward either inhibition (Haider et al., 2013) or excitation (Taub et al., 2013) as animals recover from anesthesia. It is plausible that the large changes in SF tuning we observed in alert monkeys could be disrupted under anesthesia.

Previous reports have suggested that the balance of excitation and inhibition in cortical networks plays an important role in shaping selectivity for stimulus features. Feedforward cortical excitation is often thought to play a dominant role in shaping cortical tuning (Barlow, 1953; Hubel and Wiesel, 1959, 1968; Ferster, 1996; Riesenhuber and Poggio, 2002; Priebe & Ferster, 2008).

Cortical inhibition is often thought to play only a modulatory role: by sharpening the tuning functions of individual neurons and not by changing the peaks of tuning functions (Sillito, 1979; Sato et al., 1996; Kyriazi et al., 1996; Crook et al., 1997; Ringach et al., 1997; Sompolinsky & Shapley, 1997; Wang et al., 2000; Poo & Isaacson, 2009; Katzner et al., 2011; Isaacson & Scanziani, 2011).

Rubin et al. (2015) studied SF tuning of single neurons in the primary visual cortex of anesthetized ferrets and they, too, found a significant, although small, change of preferred SF with contrast. In 72% of studied neurons, preferred SF drifted to higher SF, and in the remaining 28%, the preferred SF either decreased or did not change. The authors developed a model of the distributed neural circuit stabilized by inhibition, based on the framework introduced by Wilson & Cowan (1972, 1973; also see Teich & Qian, 2003; Ozeki et al., 2009; Ahmadian et al., 2013; Rubin et al., 2015; Miller 2016). Connections between excitatory cells were limited to nearest- and next-to-nearest neighbors, while inhibitory cells in different nodes were not connected. The model predicted an increase of SF preference with contrast. To account for this pattern of results Rubin et al. proposed that cell tuning is dominated by external excitatory inputs at low stimulus strengths and by inhibitory influences in the local circuitry at high stimulus strengths.

In a different computational study, Gepshtein et al (2018) developed a model of the distributed canonical circuit, which had reciprocally and recurrently connected excitatory and inhibitory cells, as in Rubin et al., but the connections between excitatory and inhibitory cells were limited to nearest neighbor alone. These investigators found that such a distributed circuit is characterized by an intrinsic preference for SF, and that the preferred SF depends on stimulus contrast. Increasing contrast generally causes a change in the preferred SF, while the direction of change depends on whether the circuit is dominated by excitation or inhibition. The amount of change also depends on stimulus TF, forming a pattern similar to that shown in Figure 6.

Taken together, our results and results of theoretical studies of cortical selectivity (Rubin et al., 2015; Gepshtein et al, 2018) support the notion that SF tuning depends on the balance of excitation and inhibition in the network and that a slight imbalance can cause a change in network selectivity. The experimental and modeling results suggest furthermore that inhibition does more than sharpen neuronal tuning; in alert animals, inhibition can also change the peak of tuning.

Interaction of stimulus spatial and temporal frequency in cortical tuning

Several previous studies investigated how contrast affects TF preferences of sensory neurons. In cat retinal ganglion cells, peaks of TF tuning curves were found to shift with contrast to higher

values (Shapley & Victor, 1978). Similar results have been reported for area V1 of anesthetized ferrets (Alitto & Usrey, 2004). Foster et al. (1985) studied tuning across a range of SF and TF combinations in V1 of anesthetized macaque monkeys. They found that SF tuning was independent of TF. Following results of these and other studies (Saul & Humphrey, 1992; Hawken et al., 1996; Yu et al., 2010), the question of how stimulus contrast and stimulus TF affect tuning in the cortex has remained unresolved.

In previous studies, explanations for the interaction between effects of stimulus SF and TF on neuronal tuning were sought in terms of feedforward inputs from two major neural pathways with distinct response properties: magnocellular (M) and parvocellular (P) (Hendrickson et al., 1978; Casagrande & Kaas, 1994; Callaway, 1998; Chatterjee & Callaway, 2003; Nassi et al., 2006; Nassi & Callaway, 2009). Notably, Nassi et al (2006) found that both pathways contribute to neuronal responses in area MT. The M pathway is most responsive to fast moving stimuli that correspond to the temporal frequencies between 10 and 20 Hz (Derrington & Lennie, 1984). The M pathway also prefers spatial frequencies below 1 c/deg (Merigan et al., 1991a; Skottun, 2000). The P pathway prefers slow moving and static stimuli and thus responds better to temporal frequencies below 10 Hz (Livingstone & Hubel, 1988; Derrington & Lennie, 1984).

How do these findings relate to our results? It is clear from Figure 8 that, for temporal frequencies above 8 Hz, the means of preferred SFs at low and high contrasts are similar to one another, and they happen to dwell below 1 c/deg. Here our data are consistent with previous findings that the M pathway dominates visual processing at higher TF. It is also clear from Figure 8 that means of peak SF at high and low contrasts diverge below 8 Hz: the differences of peak SF at high and low contrasts are larger at low TF. If the P pathway mediated neuronal responses below 8 Hz for all contrasts, we would not expect that SF preferences would be different at low and high contrasts. Are different neural mechanisms responsible for perception of stimuli at high and low contrasts when TF is low? Indeed, at contrasts above 10%, the P pathway is expected to be active (Green et al, 2008) making it likely that the P pathway dominates at low TF and high contrasts (red squares in Figure 8A, B). It is unclear what mechanism is responsible for reduction of SF preference as low TF and low contrasts (open and black squares at low TF in Figure 8). According to the evidence of the contributions of M and P pathways to cortical selectivity, it is unlikely that this mechanism resides within the M pathway because the latter is expected to be active only at high TFs. However, based on our results for low TF, and also the fact that the M pathway responds selectively to low contrasts and saturates at 16-32% contrast, it is possible that the M pathways is active at low contrasts and low TFs. In summary, our data suggests that the M

pathway is active at all contrasts above 8 Hz. Below 8 Hz, both M and the P pathway are active, with the M pathway dominating at low contrasts and the P pathway dominating at high contrasts.

Some of our results agree with the prevailing view of cortical tuning as a feedforward process. In this view, certain features of cortical selectivity are inherited through feedforward connections from upstream sensory cortices. For example, area MT is thought to inherit direction tuning and SF tuning through feedforward connections from area V1 (Movshon & Newsome, 1996; Priebe et al., 2006). On the other hand, the modeling results described in the previous section suggest that flexible selectivity can arise independently in each cortical area, rather than being a property inherited from upstream areas. For example, studies have found that direction selectivity in MT remains partially intact after V1 lesions (Rodman et al., 1989, Girard et al., 1992) suggesting that MT might be able to develop some of its selectivity in the absence of V1 input.

Circuit-centered vs. cell-centered views on cortical tuning

As the receptive field was originally conceived, *individual* neurons are thought to function as filters, tuned to a limited range of stimuli. Tuning was thought to be largely shaped by feedforward connections ascending through a hierarchy of cortical areas (Barlow, 1953; Hubel and Wiesel, 1959, 1968; Ferster, 1996, Priebe & Ferster, 2008, Riesenhuber and Poggio, 2002). This view has been previously challenged by evidence of adaptation and contextual modulation. In adaptation, sustained exposure to a new ensemble of stimuli can alter neuronal tuning (Albrecht et al., 1984; Peterson et al., 1985; Kohn et al., 2003; Krekelberg et al. 2006, Gepshtein et al., 2013). In contextual modulation, a stimulus presented outside of a neuron's classical receptive field can modify the neuron's response to stimuli inside of the receptive field (Stoner & Albright, 2002). Next, we argue that our results present a challenge to the classical picture, from both computational and physiological perspectives.

Computationally, it is useful to consider our results on a continuum between the two extreme views of neuronal selectivity: circuit-driven and input-driven. From the circuit-driven perspective, selectivity of individual cells is fully determined by circuit connectivity, even as these properties are revealed by measuring characteristics of individual cells. From the input-driven perspective, selectivity of individual cells is fully determined by feed-forward connections, and local circuitry has only a limited, modulatory role. Between these extreme points of views on the genesis of neuronal selectivity, it is possible that different types of selectivity are determined by different processes. The interaction between stimulus contrast and selectivity for SF could arise in the local

circuit – in a process similar to that captured by the model of Gepshtein et al. (2018) – independent of other types of selectivity determined by feed-forward connections.

Physiologically, our recordings from neurons in area MT are consistent with predictions of the generalized model of canonical cortical computation, in that SF tuning of MT neurons strongly depended on stimulus contrast. We measured responses of 139 isolated MT neurons in two fixating macaque monkeys at multiple spatiotemporal frequencies and contrasts of luminance gratings and found that neurons were tuned to different spatial frequencies at different stimulus contrasts, consistent with our model predictions. Our results lead to specific predictions about how the ratio of cortical inhibition to excitation yields to changes in SF tuning. These predictions will be tested in future experiments.

CONCLUSIONS

We found that spatial frequency tuning of MT neurons in alert monkeys depends on the luminance contrast and temporal frequency of stimulation. As contrast increases, the peak of tuning shifts towards lower or higher spatial frequencies, more often the latter than the former. The changes in the peak of spatial frequency tuning are largest at low temporal frequency, and they decrease as temporal frequency increases. Our results taken together with results of theoretical studies of cortical selectivity (e.g., Rubin et al., 2015, Gepshtein et al., 2018) suggest that a change in the balance of excitation and inhibition is likely to cause a contrast dependent change in cortical preference to spatial frequency. These changes in neuronal preference across contrast, spatial frequency and temporal frequency suggest that contextual modulations, defined broadly in terms of nonlinear interactions of stimulus dimensions, are more pervasive than previously thought.

ACKNOWLEDGEMENTS

This study was supported in part by a research grant from the National Eye Institute (R01 EY018613). Core research support was provided by an NEI Core Grant for Vision Research (P30 EY019005). Additional support was provided by the GemCon Family Foundation and Conrad T. Prebys. We are grateful to Dinh Diep for exceptional technical assistance during the course of these experiments.

AUTHOR CONTRIBUTIONS

Conceptualization, A.S.P., S.G. and T.D.A.; Methodology, A.S.P., S.G., S.S. and T.D.A.; Software, A.S.P., S.G. and S.S.; Validation, A.S.P., S.G. and S.S.; Formal Analysis, A.S.P., S.G.

and S.S.; Investigation, A.S.P.; Resources, T.D.A.; Data Curation, A.S.P.; Writing-Original Draft, A.S.P.; Writing-Review & Editing, A.S.P., S.G. and T.D.A.; Visualization, A.S.P., S.G., S.S. and T.D.A.; Supervision, S.G. and T.D.A.; Project Administration, A.S.P., S.G. and T.D.A.; Funding Acquisition, S.G. and T.D.A.

DECLARATION OF INTERESTS

The authors declare no competing interests.

REFERENCES

Ahmadian, Y., Rubin, D.B., and Miller, K.D. (2013). Analysis of the stabilized supralinear network. Neural Comput. *25*, 1994–2037.

Albrecht, D.G., Farrar, S.B., and Hamilton, D.B. (1984). Spatial contrast adaptation characteristics of neurones recorded in the cat's visual cortex. J. Physiol. *347*, 713–739.

Albrecht, D.G. (1995). Visual cortex neurons in monkey and cat: effect of contrast on the spatial and temporal phase transfer functions. Vis Neurosci *12*, 1191–1210.

Albright, T.D., and Stoner, G.R. (2002). Contextual Influences on Visual Processing. Annu. Rev. Neurosci. *25*, 339–379.

Albright, T.D. (2012). On the Perception of Probable Things: Neural Substrates of Associative Memory, Imagery, and Perception. Neuron *74*, 227–245.

Albright, T.D. (2015). Perceiving. Daedalus. *144:1*, 22-41

Alkire, M.T., Hudetz, A.G., and Tononi, G. (2009). Consciousness and Anesthesia NIH Public Access. *322*, 876–880.

Alitto, H. J., and Usrey, W. M. (2004). Influence of contrast on orientation and temporal frequency tuning in ferret primary visual cortex. J. Neurophysiol. *91(6)*, 2797-2808.

Allman, J., Miezin, F., and McGuinness, E. (1985). Direction-and velocity-specific responses from beyond the classical receptive field in the middle temporal visual area (MT). Perception. *14(2)*, 105-126.

Barlow, B.Y.H.B. (1953). Action potentials from the frog's retina. J. Physiol. *119*, 58–68.

Barlow, H. B. (1972). Single units and sensation: a neuron doctrine for perceptual psychology? Perception, *1(4)*, 371-394.

Bishop, P. O., Coombs, J. S., and Henry, G. H. (1973). Receptive fields of simple cells in the cat striate cortex. J. Physiol. *231(1)*, 31-60.

Bullier, J., Hupé, J.M., James, A., and Girard, P. (1996). Functional interactions between areas V1 and V2 in the monkey. J. Physiol. Paris *90*, 217–220.

Buzsaki, G. (2006). Rhythms in the brain. Oxford University Press.

Callaway, E. M. (1998). Local circuits in primary visual cortex of the macaque monkey. Annu. Rev. Neurosci, *21(1)*, 47-74.

Casagrande, V. A., and Kaas, J. H. (1994). The afferent, intrinsic, and efferent connections of primary visual cortex in primates. Primary visual cortex in primates *(pp. 201-259)*. Springer, Boston, MA.

Chatterjee, S., and Callaway, E. M. (2003). Parallel colour-opponent pathways to primary visual cortex. Nature. *426(6967)*, 668.

Crook, J.M., Kisvárday, Z.F., and Eysel, U.T. (1997). GABA-induced inactivation of functionally characterized sites in cat visual cortex (area 18): effects on direction selectivity. J. Neurophysiol. *75*, 2071–2088.

Das, A., and Gilbert, C.D. (1999). Topography of contextual modulations mediated by short-range interactions in primary visual cortex. Nature *399*, 655–661.

Derrington, A.M., and Lennie, P. (1984). Spatial and temporal contrast sensitivities of neurons in lateral geniculate nucleus of macaque. J. Physiol. *357*, 219–240.

Dobkins, K. R., and Albright, T. D. (1994). What happens if it changes color when it moves?: the nature of chromatic input to macaque visual area MT. J. Neurosci. *14(8)*, 4854-4870.

Dong, D. W. (2001). Spatiotemporal inseparability of natural images and visual sensitivities. Motion Vision-Computational, Neural & Ecological Constraints. 371-380.

Duncan, R. O., Albright, T. D., and Stoner, G. R. (2000). Occlusion and the interpretation of visual motion: perceptual and neuronal effects of context. J. Neurosci. *20(15)*, 5885-5897.

Ferster, D. (1996). Is neural noise just a nuisance? Science *273*, 1812.

Fleet, D. J., and Jepson, A. D. (1985). Velocity extraction without form interpretation. Proceedings of the IEEE workshop on Computer Vision. 179-185.

Foster, K. H., Gaska, J. P., Nagler, M., and Pollen, D. A. (1985). Spatial and temporal frequency selectivity of neurones in visual cortical areas V1 and V2 of the macaque monkey. J. Physiol. *365(1)*, 331-363.

Gepshtein, S., Lesmes, L.A., and Albright, T.D. (2013). Sensory adaptation as optimal resource allocation. Proc. Natl. Acad. Sci. *110*, 4368–4373.

Gepshtein, S., Pawar, A.S., Savel'ev, S. and Albright, T.D. (2015). Neural wave interference and intrinsic tuning in distributed excitatory-inhibitory networks. arXiv, arXiv:XXXXXXX.

Girard, P., Salin, P. A., and Bullier, J. (1992). Response selectivity of neurons in area MT of the macaque monkey during reversible inactivation of area V1. J. Neurophysiol. *67(6)*, 1437-1446.

Green, M. F., Butler, P. D., Chen, Y., Geyer, M. A., Silverstein, S., Wynn, J. K., Yoon, J. H. and Zemon, V. (2008). Perception measurement in clinical trials of schizophrenia: promising paradigms from CNTRICS. Schizophrenia bulletin. *35(1)*, 163-181.

Haider, B., Häusser, M., and Carandini, M. (2013). Inhibition dominates sensory responses in the awake cortex. Nature *493*, 97–100.

Hawken, M. J., Shapley, R. M., and Grosof, D. H. (1996). Temporal-frequency selectivity in monkey visual cortex. Vis. Neurosci. *13(3)*, 477-492.

Hendrickson, A. E., Wilson, J. R., and Ogren, M. P. (1978). The neuroanatomical organization of pathways between the dorsal lateral geniculate nucleus and visual cortex in Old World and New World primates. J. Comp. Neurol. *182(1)*, 123-136.

Holub, R.A., and Morton-Gibson, M. (1981). Response of Visual Cortical Neurons of the cat to moving sinusoidal gratings: response-contrast functions and spatiotemporal interactions. J. Neurophysiol. *46*, 1244–1259.

Huang, X., Albright, T. D., and Stoner, G. R. (2007). Adaptive surround modulation in cortical area MT. Neuron, *53(5)*, 761-770.

Hubel, D.H., and Wiesel, T.N. (1959). Receptive fields of single neurones in the cat's striate cortex. J. Physiol. *148*, 574–591.

Hubel, D. H., and Wiesel, T. N. (1962). Receptive fields, binocular interaction and functional architecture in the cat's visual cortex. J. Physiol. *160(1)*, 106-154.

Hubel, D.H., and Wiesel, T.N. (1968). Receptive Fields and Functional Architecture of monkey striate cortex. J. Physiol. *195*, 215–243.

Hudetz, A. G. (2008). "Are we unconscious during general anesthesia?" International anesthesiology clinics. *46(3)*: 25-42.

Hupe´, J. M., James A. C., Payne B. R., Lomber, S.G., Girard, P. and Bullier, J. (1998). Cortical feedback improves discrimination between figure and background by V1, V2 and V3 neurons. Nature *428*, 153–157.

Isaacson, J.S., and Scanziani, M. (2011). How inhibition shapes cortical activity. Neuron *72*, 231–243.

Katzner, S., Busse, L., and Carandini, M. (2011). GABAA Inhibition Controls Response Gain in Visual Cortex. J. Neurosci. *31*, 5931–5941.

Kohn, A., and Movshon, J.A. (2003). Neuronal adaptation to visual motion in area MT of the macaque. Neuron *39*, 681–691.

Krekelberg, B., van Wezel, R.J.A., Albright, T.D. (2006). Interactions between Speed and Contrast Tuning in the Middle Temporal Area: Implications for the Neural Code for Speed. J. Neurosci. *26*, 8988–8998.

Kyriazi, H.T., Carvell, G.E., Brumberg, J.C., and Simons, D.J. (1996). Quantitative effects of GABA and bicuculline methiodide on receptive field properties of neurons in real and simulated whisker barrels. J. Neurophysiol. *75*, 547–560.

Li, W., Piëch, V., and Gilbert, C. D. (2006). Contour saliency in primary visual cortex. Neuron *50*, 951-962.

Livingstone, M., and Hubel, D. (1988). Segregation of form, color, movement, and depth: anatomy, physiology, and perception. Science. *240(4853)*, 740-749.

Merigan, W. H., Byrne, C. E., and Maunsell, J. H. (1991). Does primate motion perception depend on the magnocellular pathway? J. of Neurosci*. 11(11)*, 3422-3429.

Miller, K.D. (2016). Canonical computations of cerebral cortex. Curr. Opin. Neurobiol. 37, 75–84.

Mountcastle, V. B. (1957). Modality and topographic properties of single neurons of cat's somatic sensory cortex. J. Neurophysiol. *20(4)*, 408-434.

Movshon, J. A., Thompson, I. D., and Tolhurst, D.J. (1978). Spatial and temporal contrast sensitivity of neurones in areas 17 and 18 of the cat's visual cortex. J. Phsyiol., *283*, 101-120.

Movshon, J. A., and Newsome, W. T. (1996). Visual response properties of striate cortical neurons projecting to area MT in macaque monkeys. J. Neurosci. *16(23)*, 7733-7741.

Nassi, J. J., Lyon, D. C., and Callaway, E. M. (2006). The parvocellular LGN provides a robust disynaptic input to the visual motion area MT. Neuron. *50(2)*, 319-327.

Nassi, J. J., and Callaway, E. M. (2009). Parallel processing strategies of the primate visual system. Nat. Rev. Neurosci. *10(5)*, 360.

Ozeki, H., Finn, I.M., Schaffer, E.S., Miller, K.D., and Ferster, D. (2009). Inhibitory Stabilization of the Cortical Network Underlies Visual Surround Suppression. Neuron 62, 578–592.

Pack, C. C., Hunter, J. N., and Born, R. T. (2005). Contrast dependence of suppressive influences in cortical area MT of alert macaque. J. Neurophysiol. *93(3)*, 1809-1815.

Petersen, S.E., Baker, J.F., and Allman, J.M. (1985). Direction-specific adaptation in area MT of the owl monkey. Brain Res. *346*, 146–150.

Poo, C., and Isaacson, J.S. (2009). Odor Representations in Olfactory Cortex: “Sparse” Coding, Global Inhibition, and Oscillations. Neuron *62*, 850–861.

Priebe, N.J., Cassanello, C.R., and Lisberger, S.G. (2003). The neural representation of speed in macaque area MT/V5. J. Neurosci. *23*, 5650–5661.

Priebe, N.J., Lisberger, S.G., and Movshon, J.A. (2006). Behavioral/Systems/Cognitive Tuning for Spatiotemporal Frequency and Speed in Directionally Selective Neurons of Macaque Striate Cortex. J. Neurosci. *26*, 2941–2950.

Priebe, N.J., and Ferster, D. (2008). Inhibition, Spike Threshold, and Stimulus Selectivity in Primary Visual Cortex. Neuron *57*, 482–497.

Riesenhuber, M., and Poggio, T. (2002). Neural mechanisms of object recognition. Curr. Opin. Neurobiol. *12(2)*, 162-168.

Ringach D L, Hawken M J, S.R. (1997). Dynamics of orientation tuning in macaque primary visual cortex. J. Clin. Microbiol. J. Gen. Virol *30*, 947–950.

Rodman, H. R., Gross, C. G., and Albright, T. D. (1989). Afferent basis of visual response properties in area MT of the macaque. I. Effects of striate cortex removal. J. Neurosci. *9(6)*, 2033-2050.

Rubin, D.B., VanHooser, S.D., and Miller, K.D. (2015). The stabilized supralinear network: A unifying circuit motif underlying multi-input integration in sensory cortex. Neuron *85*, 402–417.

Sato, H., Katsuyama, N., Tamura, H., Hata, Y., and Tsumoto, T. (1996). Mechanisms underlying orientation selectivity of neurons in the primary visual cortex of the macaque. J. Physiol. *494(Pt 3)*, 757–771.

Saul, A. B., and Humphrey, A. L. (1992). Temporal-frequency tuning of direction selectivity in cat visual cortex. Vis. Neurosci. *8(4)*, 365-372.

Sceniak, M.P., Hawken, M.J., and Shapley, R. (2002). Contrast-dependent changes in spatial frequency tuning of macaque V1 neurons: effects of a changing receptive field size. J. Neurophysiol. *88*, 1363–1373.

Schlack, A., and Albright, T. D. (2007). Remembering visual motion: neural correlates of associative plasticity and motion recall in cortical area MT. Neuron. *53(6)*, 881-890.

Shapley, R. M., and Victor, J. D. (1978). The effect of contrast on the transfer properties of cat retinal ganglion cells. J. Physiol. *285(1)*, 275-298.

Sillito, A.M. (1979). Inhibitory mechanisms influencing complex cell orientation selectivity and their modification at high resting discharge levels. J. Physiol., *289*, 33–53.

Skottun, B. C. (2000). The magnocellular deficit theory of dyslexia: the evidence from contrast sensitivity. Vis. Res. *40(1)*, 111-127.

Sompolinsky, H. and Shapley, R. (1997). New perspectives on the mechanisms for orientation selectivity. Curr. Opin. Neurobiol. *7*, 514–522.

Stoner, G. R., and Albright, T. D. (1992). Neural correlates of perceptual motion coherence. Nature. *358(6385)*, 412.

Albright, T. D., and Stoner, G. R. (2002). Contextual influences on visual processing. Annu. Rev. Neurosci. *25(1)*, 339-379.

Supèr, H., Spekreijse, H., and Lamme, V. A. (2001). Two distinct modes of sensory processing observed in monkey primary visual cortex (V1). Nat. Neurosci. *4*, 304–310.

Tanaka, K., Hikosaka, K., Saito, H. A., Yukie, M., Fukada, Y., and Iwai, E. (1986). Analysis of local and wide-field movements in the superior temporal visual areas of the macaque monkey. J. Neurosci. *6(1)*, 134-144.

Teich, A. F., andjai Qian, N. (2003). Learning and adaptation in a recurrent model of V1 orientation selectivity. J. Neurophysiol. *89(4)*, 2086-2100.

Taub, A.H., Katz, Y., and Lampl, I. (2013). Cortical Balance of Excitation and Inhibition Is Regulated by the Rate of Synaptic Activity. J. Neurosci. *33*, 14359–14368.

Wang, J., Caspary, D., and Salvi, R.J. (2000). GABA-A antagonist causes dramatic expansion of tuning in primary auditory cortex. Neuroreport *11*, 1137–1140.

Wilson, H.R., and Cowan, J.D. (1972). Excitatory and Inhibitory Interactions in Localized Populations of Model Neurons. *12(1),* 1-24.

Wilson, H.R., and Cowan, J.D. (1973). A mathematical theory of the functional dynamics of cortical and thalamic nervous tissue. Biol. Cybern. *13*, 55–80.

Wilson, H. R. (1999). Spikes, decisions, and actions: the dynamical foundations of neurosciences.

Yu, H. H., Verma, R., Yang, Y., Tibballs, H. A., Lui, L. L., Reser, D. H., and Rosa, M. G. (2010). Spatial and temporal frequency tuning in striate cortex: functional uniformity and specializations related to receptive field eccentricity. Eur. J. Neurosci., *31(6)*, 1043-1062.

METHODS

Contact for reagent and resource sharing

Further information and requests for resources and reagents should be directed to and will be fulfilled by the Lead Contact, Ambarish Pawar (ambarish@salk.edu).

Experimental model

Animals

Two adult male rhesus monkeys (Macaca mulatta) of ages 11 and 12 were used in this study. Both monkeys weighed between 11 and 13 kg during the course of the experiments. Both monkeys were single housed in steel cages. Experimental protocols were approved by the Salk Institute Animal Care and Use Committee, and conform to US Department of Agriculture regulations and to the National Institutes of Health guidelines for the humane care and use of laboratory animals.

Surgical preparation

Procedures for surgery and wound maintenance have been described in detail elsewhere (Dobkins and Albright, 1994). Briefly, a head post and a recording cylinder were affixed to the skull using stainless steel rails and screws (Synthes) and dental acrylic. Cranial magnetic resonance imaging (MRI) scans performed before surgery aided positioning of the recording chamber above MT. After surgical recovery and attainment of criterion performance on a visual fixation task (see below), a craniotomy was performed to allow for electrode passage into area MT. All surgical procedures were performed under sterile conditions, and animals were given prophylactic antibiotics (three doses of 30 mg/kg Keflin during surgery at 2 hr intervals) and postsurgical analgesics (buprenophorine, 0.03 mg/kg, i.m., every 12 hr for 3 d).

Method details

Behavioral task

Monkeys were seated in a standard primate chair (Crist Instruments) with head post rigidly supported by the frame of the chair. Animals were required to fixate a small (0.2° diameter) fixation target in the presence of moving visual stimuli for the duration of each trial (500-2000 msec). The

target was presented on a video display at a viewing distance of 57 cm. Eye position was sampled at 60 Hz using an infrared video-based system (IScan, Burlington, MA). The eye position data were monitored and recorded with the CORTEX program (Laboratory of Neuropsychology, National Institute of Mental Health, Bethesda, MD), which was also used to implement the behavioral paradigm and to control stimulus presentation. After successful fixation (i.e., the maintenance of eye position within a 2° window centered on the fixation target) throughout the trial, animals were given a small (0.15 cc) juice reward.

Apparatus

All visual stimuli were generated in Matlab (Mathworks, Natick) software using a high-resolution graphics display controller (Quadro Pro Graphics card, 1024 × 768 pixels, 8 bits/pixel) operating in a Pentium class computer. In the experiments with monkeys, stimuli were displayed on a 21-inch monitor (75 Hz, non-interlaced, 1024 × 768 pixels; model GDM-2000TC; Sony, Tokyo, Japan). The output of the video monitor was measured with a PR650 photometer (Photo-Research, Chatsworth, CA), and the voltage/luminance relationship was linearized independently for each of the three guns in the cathode ray tube. Stimuli were viewed from a distance of 57 cm in a dark room (<0.5 cd/m^2) and the mean background luminance of the monitor was 15 cd/ m^2. Monkeys were seated in a standard primate chair (Crist Instruments, Germantown, MD) with the head post rigidly supported by the chair frame.

Electrophysiological paradigm

We recorded the activity of single units in area MT using tungsten microelectrodes (3–5 MΩ; Frederick Haer Company, Bowdoinham, ME), which were driven into cortex using a hydraulic micropositioner (model 650; David Kopf Instruments, Tujunga, CA). Neurophysiological signals were filtered, sorted, and stored using the Plexon (Dallas, TX) system. We identified area MT physiologically by its characteristically high proportion of cells with directionally selective responses, receptive fields (RFs) that were small relative to those of neighboring medial superior temporal area, and its location on the posterior bank of the superior temporal sulcus. The typical recording depth agreed well with the expected anatomical location of MT that was determined from structural magnetic resonance scans.

Visual responses were recorded from 139 directionally selective MT neurons in two awake, fixating macaque monkeys (74 and 65 neurons in Monkey 1 and 2 respectively). For each MT

neuron tested, the receptive field was mapped using a white bar moving on a gray background. The preferred direction for the neuron was determined from its directional tuning curve, obtained by presenting moving black/white square gratings (1 cycles/degree, 4 Hz, 100% Michelson contrast) in eight different directions. The optimal spatiotemporal frequencies for the neuron were determined by presenting sinusoidal gratings at various spatial frequencies (range = 0.03 to 16 cycles/degree) and temporal frequencies (range = 0.25 to 32 Hz) at 100% contrast. We then measured firing rates to stimuli at five to seven different levels of luminance contrast (0.05-100%) at the preferred spatiotemporal frequencies: five spatial and one to five temporal frequencies. The number of measurements made at each spatial and temporal frequency are shown in Figure 2.

The number of trials per condition was ten. We found that ten trials per condition was a sufficient number since it allowed us to obtain reliable measures of spatial frequency tuning (Figure S1 and S2) and enabled us to measure spatial frequency tuning curves at multiple temporal frequencies within a single neuron. The sequence of events in a single trial is as follows. In each trial, the grating was turned on and stayed static on the screen for 200 ms. After 200 ms., the grating moved at a given temporal frequency for 500 ms. Firing rates reported in this paper was based on the spike counts obtained from the 500 ms. during which the grating drifted in the receptive field of the neuron being measured. The different stimulus conditions and contrasts were interleaved in random order across trials.

Most of the neurons measured in this study were between 3 and 9 degrees of the fovea in both monkeys. The stimulus size was scaled depending on eccentricity of the receptive field center from the fovea. For example, for a neuron whose receptive field location was 5 degrees from the fovea, the diameter of the stimulus was 5 degrees.

Quantification and statistical analysis

Data resampling

For each neuron, the firing rates estimated in separate trials within each frequency and contrast condition were resampled with replacement. The number of samples was equal to the number of trials in the actual experiments, which was ten. We then fitted response functions to the surrogate (resampled) data using non-parametric polynomial regression, repeated for 500 iterations of resampling, and thus estimated the errors of peak SF for each condition. The errors were then used to measure differences between peaks at different contrasts.

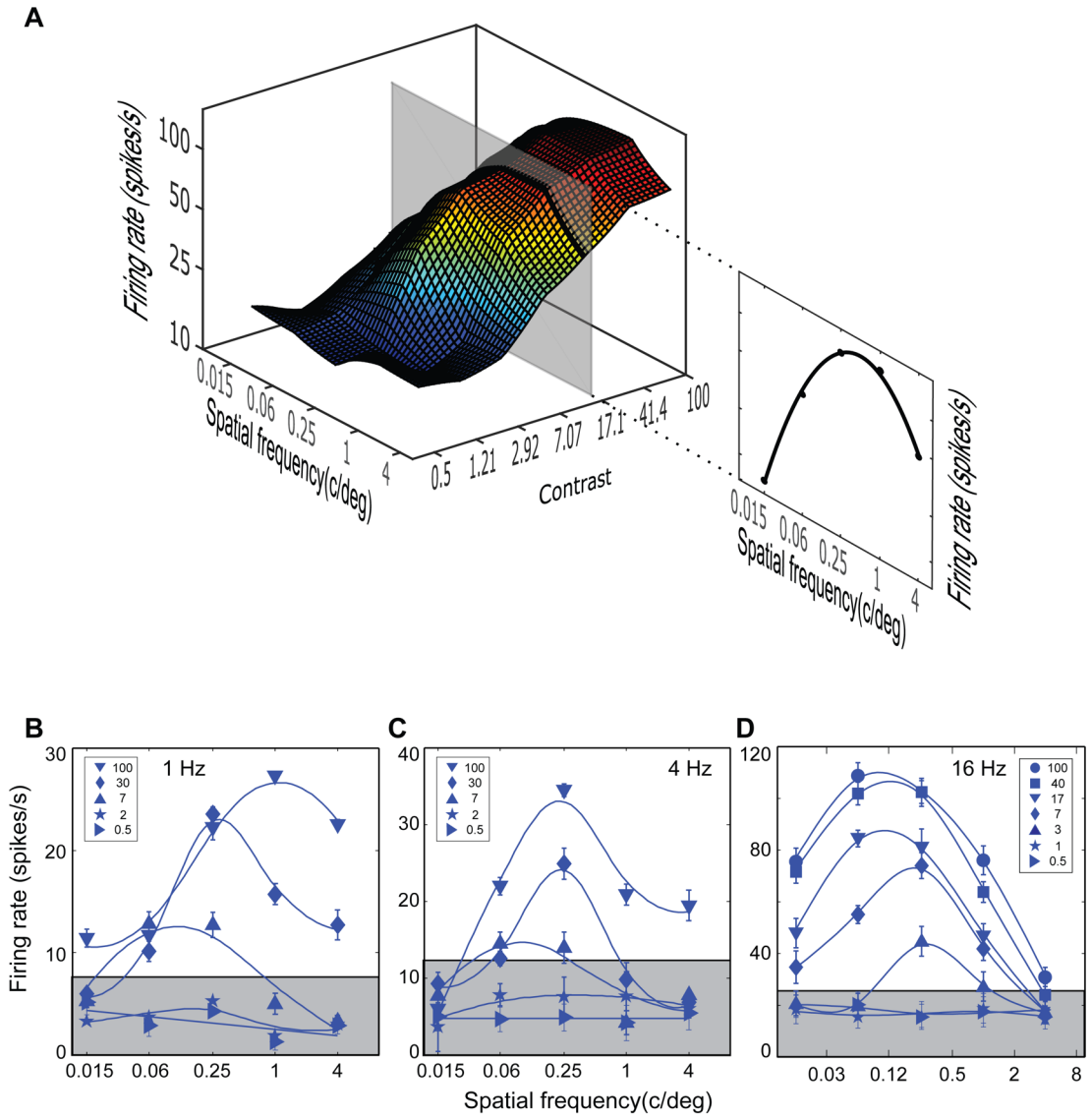

Figure 1. Response surface and response functions of MT neurons

(A) Response surface of an MT neuron. The right outset contains a vertical slice of the surface that represents the response function at the contrast of 17.1%.

(B-D) Response functions at for three different neurons, each at a different temporal frequency. Each of the blue curves represents the response function at a single contrast (%, marked in the legend). The upper edge of the shaded region represents the threshold: the contrast at which the firing rate was the mean resting rate plus one standard deviation of the resting rate.

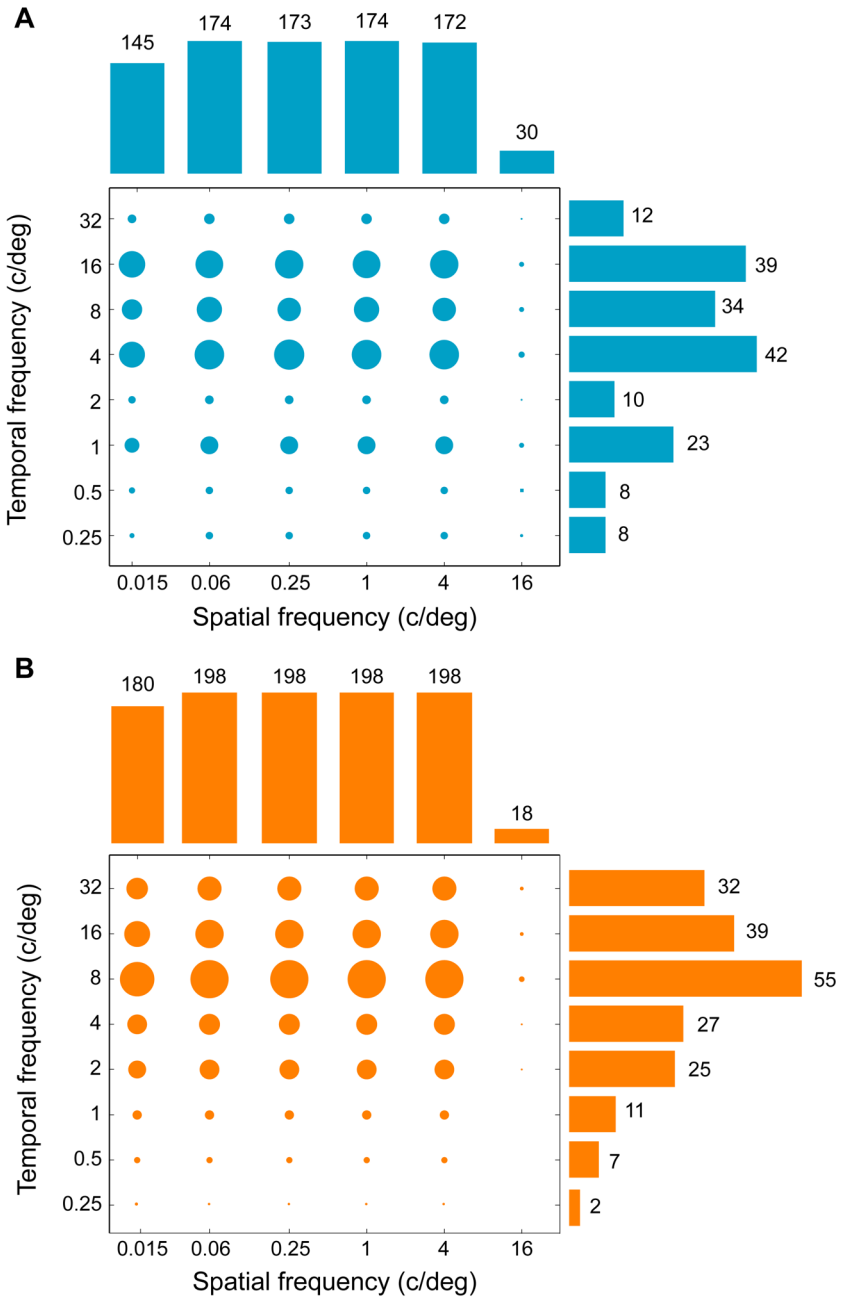

Figure 2: **Sampling distributions of stimuli**

(A) Circle sizes indicate the number of measurements performed at each spatiotemporal frequency condition for Monkey 1. The histograms at top and right of the plot describe the marginal sampling distributions of spatial and temporal stimulus frequencies.

(B) The data for Monkey 2 as in panel A.

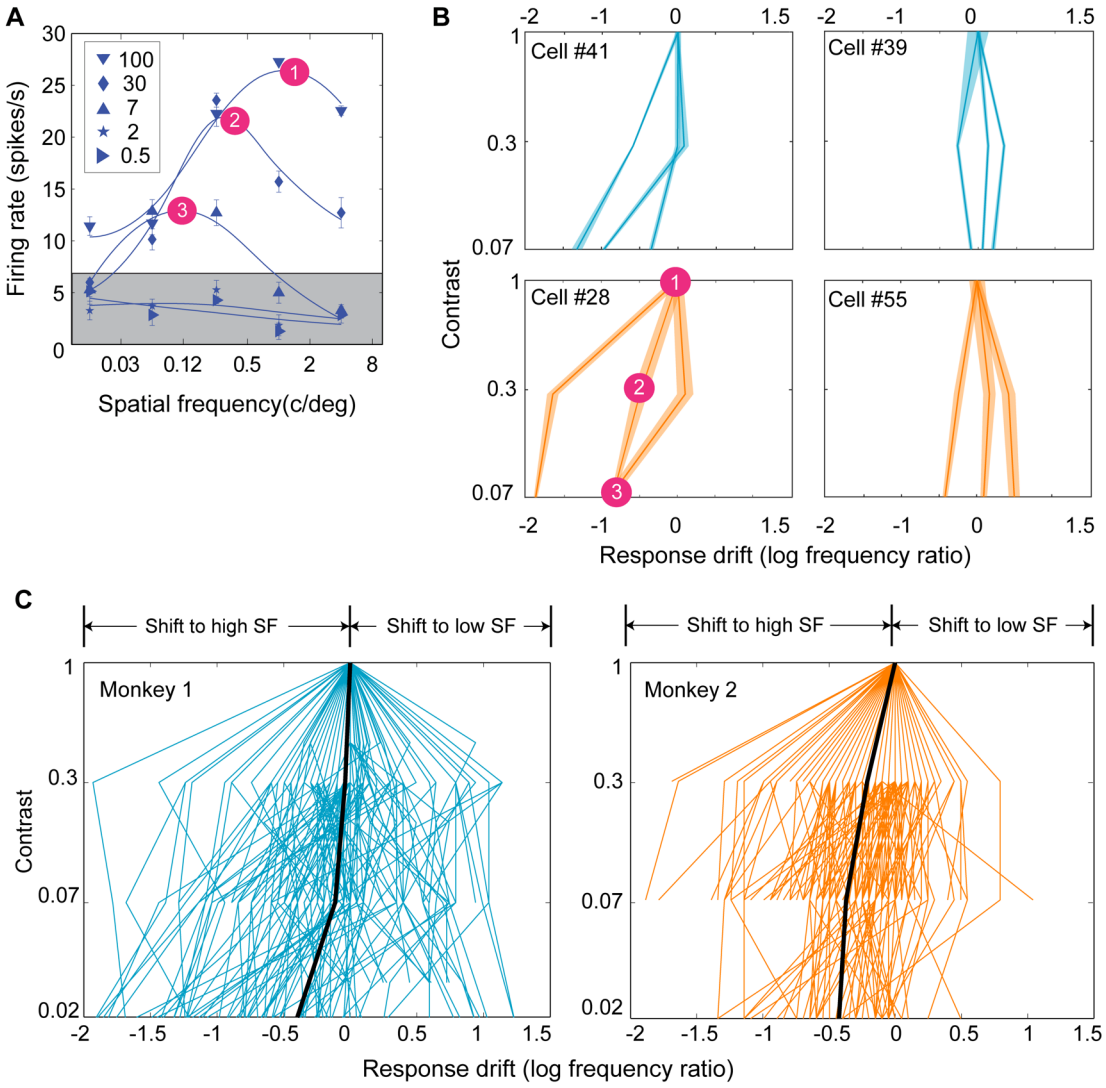

Figure 3. Drift of spatial frequency tuning with contrast

(A) Response functions from a single temporal frequency (TF) of a representative neuron. Each of the blue curves represents the response function at a single contrast (%, marked in the legend). Three values of response drift were obtained at three contrasts for this particular TF sample, as marked by the number disks (magenta, see text for details).

(B) The lines in each panel connect values of normalized peak spatial frequency (SF) across contrasts. Each line corresponds to a different TF. Response drift was defined as the log ratio of peak SF at every measured contrast above the threshold to the peak SF at the highest contrast (which always was 100% for all measured neurons). Shaded bands around each trace represent 95% confidence interval of the estimate of peak SF for each contrast (obtained using a resampling procedure described in Methods). The line connecting the numbered disks in the bottom left panel represents response drift for the neuron shown in A.

(C) Response drifts for all TFs and neurons for two monkeys. Positive and negative values of drift indicate that the preferred SF respectively increases and decreases with contrast. The slope of each line indicates the magnitude of drift. The thick black lines represent the means of response drift (sample size of at least 100).

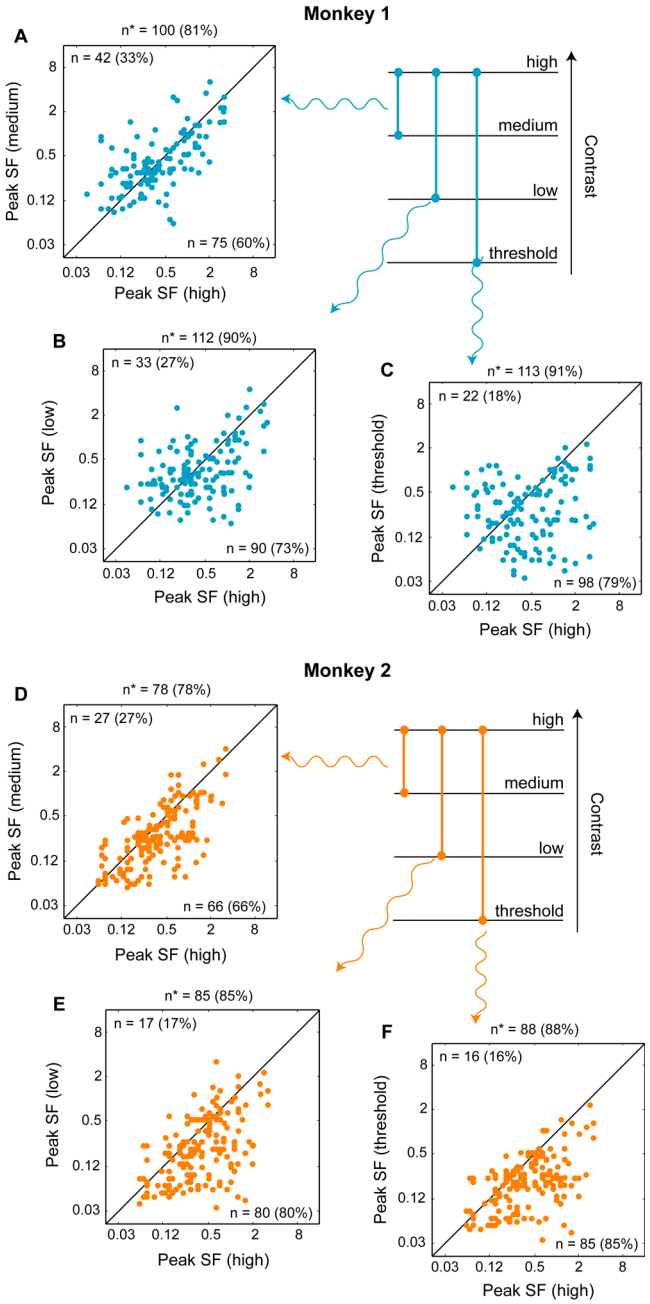

Figure 4. Spatial frequency preference across contrast

(A-C) Scatter plot of peak spatial frequencies (SF) at three contrasts: high vs. medium (A), high vs. low (B) and high vs. threshold (C) for Monkey 1. Each point represents the peak spatial frequency obtained at a certain temporal frequency. The numbers and percentages (in parentheses) in the top left and bottom right corners are the number of data points that were above or below the unit-slope diagonal. The numbers above each panel indicate the number of data points where a significant difference was found between the peaks at the given contrasts at the 99% confidence interval. (In several cases, peak responses at low contrasts were smaller than the threshold firing rate for the sample. These data were not used in panels B and C.)

(D-F) Data for Monkey 2 are plotted as in panels A-C.

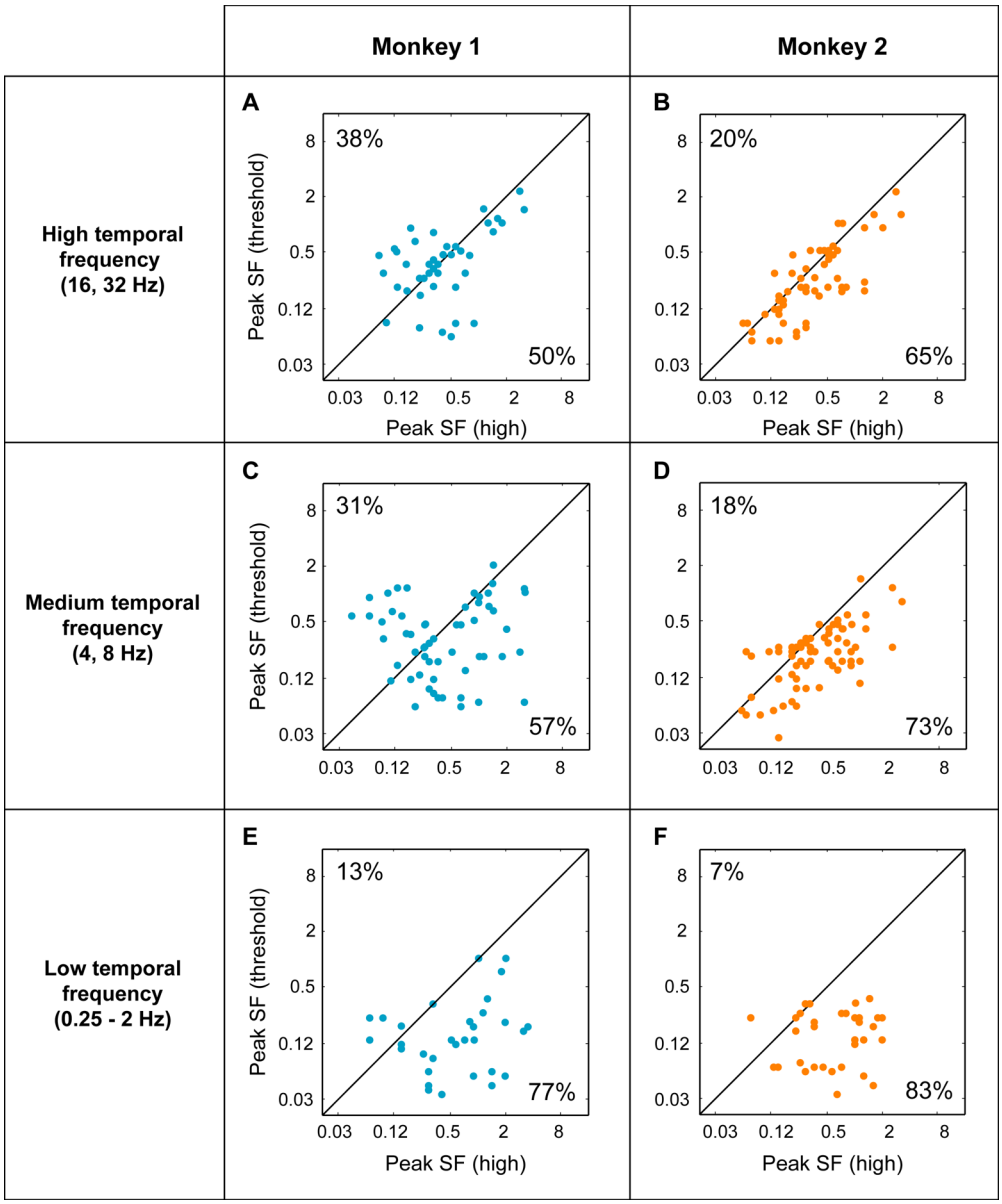

Figure 5. Spatial frequency preference across contrast separated by temporal frequency

(A-F) Scatter plot of peak spatial frequencies (SF) at high vs. threshold contrasts split into three temporal frequency (TF) bands. Each row contains data from a different TF band: high TF (A, B), medium TF (C, D) and low TF (E, F) for both monkeys.

(A, C, E) Data for Monkey 1. Each point represents the peak SF obtained at the TFs in the range indicated at left. The numbers at top left and bottom right of each plot represent percentages of the data points that fall above or below the diagonal.

(B, D, F) Data for Monkey 2 plotted as in panels A, C, and E.

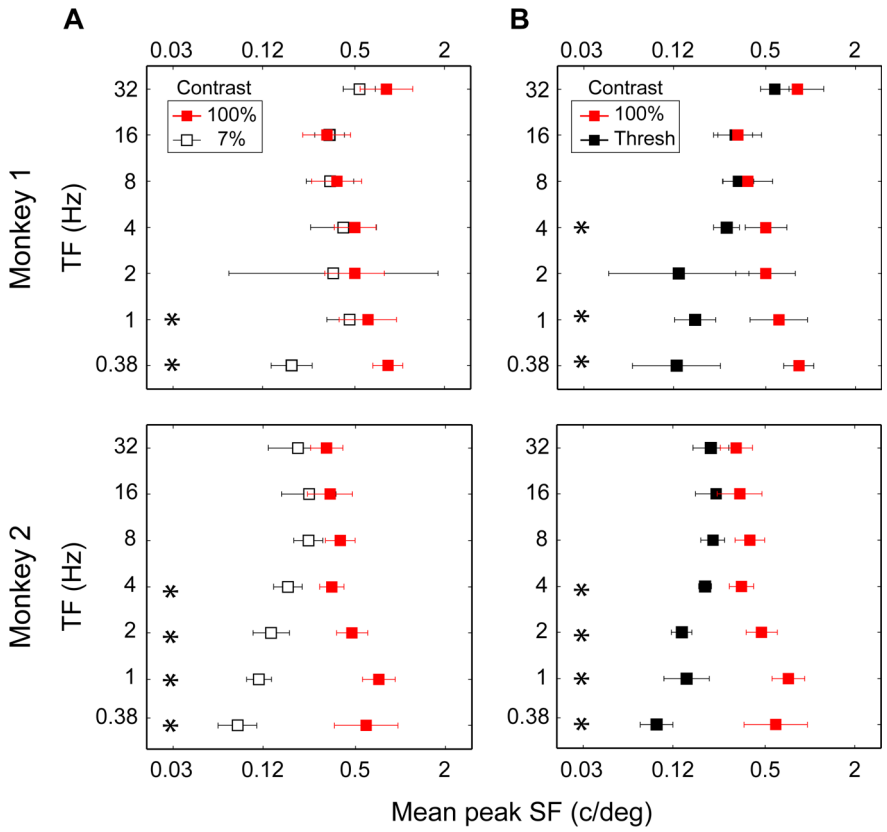

Figure 6: Interaction of spatial frequency preference and stimulus temporal frequency

(A) Comparison of preferred SF at 7% (black symbols) and 100% (red symbols) stimulus contrasts in two monkeys. Each square symbol represents the geometric mean of peak SFs. As TF increased, preferred SF monotonically increased at 7% contrast and monotonically decreased at 100% contrast. The error bars represent standard deviations of the mean.

(B) Comparison of SF tuning at the threshold contrast (black symbols) and at 100% contrast (red symbols) in two monkeys. Similar to 7% contrast (panel A), SF tuning at the threshold contrast increased with TF.

In all panels, the asterisks mark the TF conditions where the preferred SF at the two compared contrasts were significantly different from one another ($p < 0.05$).

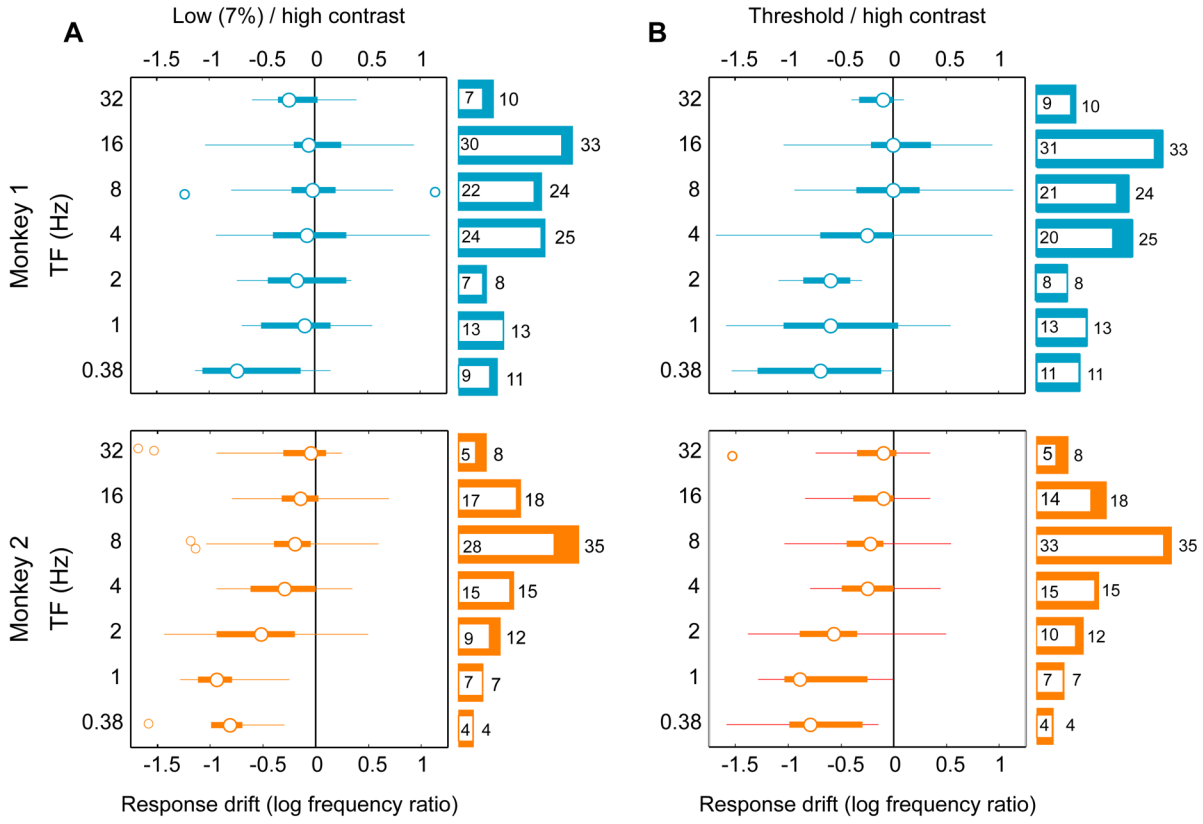

Figure 7. Drifts of peak responses across temporal frequencies

(A) Boxplot of response peak drift at different temporal frequencies. "Response drift" is decimal log ratio of peak frequencies at threshold and high contrasts. Positive and negative values of response drift indicate decrease and increase of response peak with contrast. The white circles represent the medians, box widths represent interquartile ranges, and the whiskers represent minima and maxima of the response drifts. The open circles outside the box are the outliers: response drift values that are greater than twice the interquartile range.

(B) Data for Monkey 2 are plotted as in panels A.

In all panels, the histograms represent the number of neurons from which the corresponding TFs were sampled in each monkey, cyan for Monkey 1 and orange for Monkey 2. The white areas inscribed in the colored bars represent the number of cases at which the preferred SFs at the two compared contrasts were significantly different from one another ($p < 0.01$). Data from the same neuron could contribute to up to three bars of the histogram, depending on the number of TFs ("cases") sampled from that neuron.